THE DEVELOPMENT AND APPLICATION OF AERODYNAMIC UNCERTAINTIES; AND FLIGHT TEST VERIFICATION FOR THE SPACE SHUTTLE ORBITER

Joe D. Gamble, Douglas R. Cooke, Jimmy M. Underwood
NASA-Johnson Space Center
Houston, TX

Howard W. Stone, Jr.
NASA-Langley Research Center
Hampton, VA

Donald C. Schlosser
Rockwell International
Downey, CA

ABSTRACT

The approach used in establishing the predicted aerodynamic uncertainties and the process used in applying these uncertainties during the design of the Orbiter flight control system and the entry trajectory is presented. The flight test program that was designed to verify the stability and control derivatives with a minimum of test flights is presented and a comparison of preflight predictions with preliminary flight test results is made. It is concluded that the approach used for the Orbiter is applicable to future programs where testing is limited due to time constraints or funding.

NOMENCLATURE

A	Amplitude, deg/sec or g´s
AN	Normal acceleration, g´s
Ax	Axial acceleration, g´s
Ay	Lateral acceleration, g´s
C_{ℓ_β}	Coefficient of roll due to sideslip, per deg
$C_{\ell_{\delta_a}}$	Coefficient of roll due to aileron deflection, per deg
$C_{\ell_{\delta_r}}$	Coefficient of roll due to rudder deflection, per deg
C_{n_β}	Coefficient of yaw due to sideslip, per deg
$C_{n_{\delta_a}}$	Coefficient of yaw due to aileron deflection, per deg
$C_{n_{\delta_r}}$	Coefficient of yaw due to rudder deflection, per deg
$C_{N_{\delta_e}}$	Coefficient of normal force due to elevon deflection, per deg
C_m	Pitching moment coefficient
C_{m_o}	Pitching moment coefficient at 0 angle of attack
$C_{m_{\delta_{BF}}}$	Coefficient of pitching moment due to bodyflap deflection, per deg
$C_{m_{\delta_e}}$	Coefficient of pitching moment due to elevon deflection, per deg
C_{m_α}	Coefficient of pitching moment due to angle of attack, per deg
C_{Y_β}	Coefficient of side force due to sideslip, per deg
$C_{Y_{\delta_a}}$	Coefficient of side force due to aileron deflection, per deg
$C_{Y_{\delta_r}}$	Coefficient of side force due to rudder deflection, per deg

L_B	Body length, in.
L/D	Lift-to-drag ratio
M	Mach number
T	Time, sec
V	Velocity, ft/sec
X	Body axis axial coordinate, in.
Y	Body axis lateral coordinate, in.
Z	Body axis vertical coordinate, in.
α	Angle of attack, deg
β	Sideslip angle, deg
δ_a	Aileron deflection, deg
δ_{BF}	Bodyflap deflection, deg
δ_e	Elevon deflection, deg
δ_r	Rudder deflection, deg
δ_{SB}	Speedbrake deflection, deg
σ	Standard deviation
$\bar{q}$	Dynamic pressure, psf
ω_d	Undamped natural frequency of the dutch roll oscillation
ω_ϕ	Undamped natural frequency of the numerator of ϕ/δ_a transfer function

ACRONYMS

ACIP	Aerodynamic Coefficient Identification Package
cg	Center of gravity
FCS	Flight Control System
FSL	Flight Software Laboratory
GN&C	Guidance, Navigation and Control
GPC	General purpose computer
IMU	Inertial Measurement Unit
LRU	Line replaceable unit
MMLE3	Modified maximum likelihood estimator, version 3
MXRCS	RCS roll moment
MZRCS	RCS yaw moment
POPU	Pushover Pullup Maneuver
PTI	Programmed test input
RCS	Reaction control system
SPS	Shuttle Procedures Simulator
STS	Space Transportation System
STS-1	First Flight of the Space Shuttle
STS-2	Second Flight of the Space Shuttle
WOW	Worse on worse combination of errors

INTRODUCTION

The decision to perform an orbital manned mission on the first Shuttle launch presented several challenges to the entry design community. A significant challenge was presented by the question of how to maximize safety (man rate the system) on the first flight considering the parallel development of the aerodynamics and the Flight Control System (FCS). A challenge was also presented in setting up a flight test program for a vehicle that was flying through a continuously changing environment. Finally, because of cost and operational constraints, the question of how to develop an operational vehicle with a minimum flight test program became a large challenge. This paper will address how these challenges were successfully met.

AERODYNAMIC VARIATIONS DEVELOPMENT

The challenge of maximizing safety on the first flight led to development of a reasonable estimate of maximum possible errors in the preflight predicted aerodynamics which were used to certify the FCS prior to the first flight. The best approach for the development of these errors which were called variations, was concluded to be an analysis of the wind tunnel to flight test differences of previous aircraft programs. Unfortunately, the verification of preflight predicted

aerodynamics was not a major objective of most of the previous flight test programs. This severely limited the amount of data available for conducting flight test to wind tunnel comparisons. The flight data base was further limited by restricting the comparison to those vehicles which were geometrically similar to the Orbiter. Those vehicles chosen as applicable to the Orbiter are presented in table 1. Also presented are geometric factors and other considerations pertinent to the vehicle configuration choices.

Variations were established by fairing the differences between the flight and predicted aerodynamics as a function of Mach number. The selections of the configurations and the fairing process are very subjective in nature. For this reason, a team of aerodynamicists from the various NASA centers, the Air Force and the contractors was formed to conduct the analysis and reach a consensus on variations.

The team's flight-to-predicted correlation and their recommended variations fairings are presented in reference 1. A more detailed development is presented in reference 2. The development of a less severe set of uncertainties (tolerances) based on the repeatability of wind tunnel tests is also presented in reference 1.

Reaction control jet plume interaction variation development is reviewed in reference 3.

THE CORRELATION OF AERODYNAMIC VARIATIONS

A total of 9 lateral directional coefficients (3 each beta, aileron and rudder derivatives) were defined for application to the Orbiter entry FCS verification. Use of all possible combination of signs and variations for these 9 coefficients would have resulted in an impossible number of cases to analyze and simulate. Therefore, considerable attention was devoted to identifying the more critical combination of coefficient variations for use in FCS verification.

In addition, an alternative to a worse-on-worse (WOW) analysis was desirable to provide a less demanding and possibly more realistic result for formal verification. The initial step in reducing the WOW case was to define any sign correlation that might exist between coefficient variations based on the physical relation of the coefficients.

Reference 4 presents the details involved in defining the correlation coefficients. Correlations were established for the sideslip, aileron and rudder derivatives. For the correlated coefficients, 99 percentile ellipses were established from the equation

$$1 = (1 - \rho_{xy})^{-1}\left\{\left(\frac{X}{3\sigma_x}\right)^2 - 2\rho_{xy}\left(\frac{X}{3\sigma_x}\right)\left(\frac{Y}{3\sigma_y}\right) + \left(\frac{Y}{3\sigma_y}\right)^2\right\}.$$

X and Y are the correlated coefficients, σ_x and σ_y are the standard deviations and ρ_{xy} is the linear correlation coefficient which varies between zero and one. Stated from a probability standpoint there is a one chance in a hundred that a combination of errors in X and Y would lie outside the locus of the 99 percentile ellipse.

Figure 1 presents an example of correlations in the yawing moment and rolling moment sideslip coefficients. The vector from the origin represents the nominal value for C_{n_β} and C_{ℓ_β} while the rectangle represents the 3σ variations. The different ellipses inside the rectangle show the effect of varying the correlation from 0 to a highly correlated value of .9. Results from wind tunnel tests were used to establish the correlation coefficients.

APPLICATION OF AERODYNAMIC VARIATIONS

A programmatic decision was made to use aerodynamic variations in the Orbiter FCS design evaluation and verification process. For the initial FCS design evaluation and simulation studies, a "worst on worst" combination of variations was used. For the formal entry verification at the Flight Software Laboratory (FSL) at Rockwell, variation sets were used which correlated the roll and yaw moment coefficients for the sideslip, aileron and rudder coefficients.

Because of the wide range of flight conditions the Orbiter was to encounter during the first reentry flight test, it was required to evaluate as many combinations of aerodynamic uncertainties as possible. However it was also desirable to select a more limited set of uncertainties for concentrated analysis and simulation efforts. It thus became necessary to define those aerodynamic uncertainty combinations that presented the most potential problems to the Orbiter and to make certain that the flight control system could maintain control of the Orbiter with these

combinations. In the initial FCS evaluation, a total of 26 lateral directional variation sets were evaluated in a series of almost 600 piloted simulation runs on the Shuttle Procedures Simulator (SPS) at the Johnson Space Center (JSC). These 26 cases were selected using various trim, controllability and handling qualities criteria. Based on the results of these simulation runs plus additional trim and stability analyses, a subset of 7 cases were chosen and used for the majority of the formal verification process.

Figure 2 shows a vector diagram of the aero coefficients and RCS jets for the roll and yaw axes at Mach 3.5. The numbers shown on the diagram indicate the nomenclature used for identifying the 7 cases selected for the verification process. The corners shown indicate the WOW or "rectangular" variation sets which were used in the FCS development while the ellipses represent the correlated variations. The elliptical variation sets were generally selected from points on the ellipses that were close to the rectangular counterparts. Some of the history and logic involved in the selection of the cases used for the FCS verification will now be discussed.

LCDP AND C_{n_β} DYNAMIC

A significant portion of the analysis devoted to aerodynamic variations was applied to variation sets 19 and 20. Variation set 19 represented the most severe case for the Lateral Control Departure Parameter (LCDP).[5] During the early stages of the Orbiter development, most of the reentry was performed using an all aerodynamic control concept. Prior to rudder activation which then occurred around Mach 5, the aileron was the only aerodynamic control effector for lateral directional control and trim. A reverse aileron control that required a negative value for the LCDP, $C_{n_\beta} C_{\ell_{\delta_a}} - C_{\ell_\beta} C_{n_{\delta_a}} < 0$, was utilized prior to rudder activation.[6] The lateral trim logic was also configured so that a negative value of the LCDP was required prior to rudder activation. Some of the early simulations using aerodynamic uncertainties on the aileron and beta derivatives resulted in lateral trim and controllability problems prior to rudder activation. Analysis indicated that the problem was caused by a sign change in the LCDP in the Mach 5 region. As a partial result of this problem, several changes were made to the FCS. The basic FCS design was changed from the aileron bank control to a system utilizing the yaw RCS jets to initiate bank maneuvers and the ailerons to coordinate the maneuvers prior to activation of the rudder.[7] After the rudder became active, a gradual FCS gain change produced the conventional aileron bank control with rudder coordination.

Since use of the yaw jets for trim would result in excessive propellant requirements, the aileron was still required for trim. To improve the aileron trim capability in the critical Mach region, changes were made to the angle of attack and elevon schedules. With aero variations applied, Mach 3.5 was the highest Mach number that the rudder could be considered effective and this Mach number was chosen as the activation point for the rudder. It was then considered a requirement that aileron trim be available down to Mach 3.5 with minimal yaw RCS requirements.

Figure 3 shows the sensitivity of the Orbiter LCDP to angle of attack for several Mach numbers with the worst case aero variations applied. It is obvious that in the Mach greater than 3 region an angle of attack of more then 15° is desirable in order to maintain a negative LCDP. The early flights of the Orbiter were tailored so that the angle of attack remained above 15° for Mach greater than 3.5.

Another significant factor in the LCDP is the elevon trim position. This is due to the effect of elevon position on the aileron derivatives. A desired elevon trim position of $+5^\circ$ (down) was eventually selected for STS-1 in the Mach 3-4 region. In the higher Mach region where elevon heating is a concern, the elevon was scheduled at -1 degree (up) and in the transonic region where there was some concern about hinge moments, a schedule close to zero was selected. The elevon position is maintained by the bodyflap through a feedback from the elevon which drives the bodyflap to maintain the pre-set elevon schedule.

Application of the LCDP in the Mach range from approximately 3-8 was a driver in the angle of attack, elevon and speedbrake schedules as well as the longitudinal cg choice for STS-1.

In the longitudinal axis the primary problem associated with aero uncertainties was the pitching moment uncertainty, C_{m_o} and its effect on elevon trim position. Figure 4 shows the pre STS-1 capability to position the elevon for the design cg body length extremes of 65 percent

(forward) and 67.5 percent (aft) with pitching moment variations and with the bodyflap positioned at its extreme limits to aid the desired trim. Also shown on figure 4 is the STS-1 elevon schedule. It is obvious that with C_m variations the Orbiter could not achieve the desired elevon schedule over the design range of cg's. Based on the desired elevon schedule and the effect of pitching moment variations, the STS-1 cg was selected at 66.7 percent body length. Figure 5 shows the elevon envelope at the 66.7 percent cg with C_m variations while figure 6 shows the effect of cg on the LCDP at Mach 3.5 for the worst case variation set. The cg envelope adopted for STS-1 mission rules is shown in figure 7.

Variation set 20 created the minimum value for C_{n_β} dynamic which is defined as $C_{n_\beta}\cos\alpha - C_{\ell_\beta}\sin\alpha\frac{I_z}{I_x}$. C_{n_β} dynamic is the stability term for coupled lateral directional motion and it was considered a requirement to have a stable value for this parameter throughout entry. Figure 8 shows C_{n_β} dynamic in the lower Mach region for variation set 20 for 1g flight at 7.5° α. The unaugmented C_{n_β} dynamic is unstable from about Mach 1.2 to 3.2 at these flight conditions.

The Orbiter FCS utilizes a side acceleration feedback to the rudder and yaw jets to provide stability augmentation. An approximate β feedback gain to the rudder can be computed and from this gain a rudder "augmented C_{n_β} dynamic" can be calculated. For the Mach 2 region the equivalent gain for β feedback to the rudder is approximately -1.5 to -2. Additional augmentation is provided by the yaw RCS jets and although the system is nonlinear, an approximation to an augmented C_{n_β} dynamic can be obtained which is valid for sideslip angles less than that required to fire all 4 jets (approximately 1° to 2°). The effective C_{n_β} dynamic for both rudder and RCS augmentation is shown in figure 8. Very little improvement is shown for the rudder augmentation. This is due to the small rudder effectiveness which results from the aeroelasticity effects and from application of aerodynamic variations. It is evident that the RCS provides a significant improvement. However after the jets are saturated additional augmentation is not available and there is a β limit beyond which control is not possible. For STS-1, angle of attack and dynamic pressure limits were established based on the ability of 2 yaw jets to control the Orbiter at 1.5° sideslip for the worst case aero variations. Figure 9 shows the lower angle of attack boundary established for the flight rules based on lateral trim concerns above Mach 3 and C_{n_β} dynamic concerns below Mach 3. In the Mach 2 region STS-1 had a dynamic pressure limit of 250 psf programmed into the guidance laws and the trajectory was shaped to provide ample margin above the lower alpha limits.

ADDITIONAL CRITERIA

While the aero variation sets associated with the LCDP and with C_{n_β} dynamic received considerable attention during the FCS design and verification process, other combinations of variations shown on figure 2 were also extensively analyzed. Diagrams similar to figure 2 were widely used in helping to select which variation sets to use at different flight conditions. This was particularly true of cases involving co-alignment of effectors and stability derivatives. For example, with the variation set 19, the beta and aileron vectors align which corresponds to the LCDP going to zero. This results in the loss of aerodynamic lateral trim capability and would require the use of yaw jets to trim. Variation set 19 was used for the worst case LCDP analysis. Variation set 20 was used for the minimum C_{n_β} dynamic case and results in both minimum β stability and rudder effectiveness. Variation set 20 resulted in another problem at higher Mach numbers which required a change to the FCS. At the hypersonic Mach numbers and 40° angle of attack when variations were applied to 1 yaw jet, a coalignment of the jet and β vectors occurred due to a counter clockwise rotation of the jet vector. Since the bank control is achieved through the combination of jets and β, a control criteria similar to the LCDP results. The form of this criteria used for the Orbiter was $C_{n_\beta}M_{X_{RCS}} - C_{\ell_\beta}M_{Z_{RCS}} > 0$. With one yaw jet firing a control reversal resulted which was similar to the case for the aileron control problem associated with

the LCDP. As a result of this problem, the FCS was changed so that a minimum of two yaw jets were always fired. Another case that received considerable attention was variation set 12 which is a high gain case utilizing the most stable sideslip derivatives in combination with the most effective control surfaces and jets. This case provided a balance for the low gain cases and resulted in FCS gains that covered the potential extremes in the aero variations. Case 9 was similar to case 20, but in the presence of large winds around Mach 5, a long period oscillation was observed under certain flight conditions. Offline stability analysis indicated the more negative $C_{n_{\delta_A}}$ associated with variation set 9 was resulting in a system approaching neutral stability.

In general cases 2, 11, and 23 produced less severe problems than the previously mentioned cases and were eventually dropped from the formal verification for STS-2. Case 2 was originally selected because it produced the largest value for $(\omega_\phi/\omega_d)^2$ and there was some concern about creating pilot induced oscillations (PIO) with this set of variations. However, there was no indication in any of the piloted simulations that this case produced any PIO tendencies. Case 11 was originally selected because it was thought to give the minimum value of the LCDP for the conventional aileron control mode. However, in the critical Mach region around Mach 2, case 9 usually resulted in a lower value of the LCDP. Case 23 was selected because it generated a maximum sideslip angle during the high heating region.

A problem that was observed with cases 9, 11 and 23 was an occasional tendency for the aileron and rudder to trim against each other after the rudder became active. From figure 2 it can be observed that the aileron and rudder vectors are almost co-aligned for these cases and is the probable cause for the trim problem. A procedure was utilized for STS-1 which required the crew to check the trim after the rudder became active and to trim the aileron back toward zero if a force fight resulted between the aileron and rudder.

FCS VERIFICATION PROCESS

The 570 piloted simulated runs on the Shuttle Procedures Simulation at JSC were completed in December 1977 and uncovered several significant problems when the variation sets were applied. Several changes were made to the FCS and another series of simulations were made in April and May of 1978. The modified FCS was able to maintain control of all combinations of aerodynamic variations except for one case in the Mach 6 region. This problem occurred when a variation set with minimum values of C_{n_β} dynamic was combined with large winds resulting in errors in the navigation derived angle of attack. Because angle of attack terms are present in the bank coordination logic of the FCS, errors in the angle of attack result in miscoordination during bank maneuvers and a resulting buildup in sideslip angle. If RCS jet failures occurred, control problems resulted for angle of attack errors greater than approximately 3^o. In order to accommodate this problem the flight rules for the early flights required manual bank reversals at reduced roll rates in the Mach 6 region if RCS jet failures occurred.

The formal integrated guidance, navigation and control (GN&C) verification testing began at the FSL in September 1979. A total of 35 runs were made before the simulation was suspended due to several significant problems that resulted. Forty-one flight software anomalies were identified of which 21 were related to the FCS. In general the problems occurring on the FSL had not been observed in the non integrated FCS simulations or were of a much smaller magnitude. As a result of the FSL results extensive analysis of the FCS was done to attempt to identify and correct the observed anomalies. The launch schedule slip due to the loose tile problem provided the FCS community an opportunity to perform a major review of the FCS design. Some of the problems were related to excessively large uncertainties applied to the GN&C line replaceable units (LRU) and some related to the FSL models. However some FCS changes were required to handle the aero variations and the Orbiter Software Control Board approved the change requests in April 1980.

Figure 10 shows the test matrix that was proposed for the final FCS verification.[8] The matrix includes aerodynamic uncertainties, winds, and tolerances on the GN&C LRU's. Most of the simulation runs were performed using the upper left box (nominal) and the lower right box (worst case). Figure 11 outlines the verification process that was approved by the Orbiter Configuration Control Board (CCB) prior to the final integrated verification testing at the FSL.[8]

The GN&C first was tested with nominal aerodynamics and then with the variations. If no problems occurred with worst case variations, verification was considered complete. If problems resulted with variations, the case was repeated with tolerances. If the system could not handle tolerances, a design change was required and the process repeated. A case that passed with tolerances but failed with variations resulted in a review with the aero group to discuss the validity of the specific variation case. The problem was then presented to the CCB who made the decision to either accept the risk associated with the case or to require a design change.

Formal verification was done on the FSL in August and September of 1980. The GN&C performance was greatly improved compared to the previous verification runs. A week long post simulation review by personnel from Rockwell, Honeywell, and JSC was conducted to thoroughly analyze the results of each run. A total of 16 anomalies were identified, but most of these were relatively minor and required no substantive action. The most significant problems were associated with the low C_{n_β} dynamic cases in the presence of design case winds around Mach 5. The program managers eventually accepted these cases after it was shown that the design winds for the STS-1 flight date of April resulted in less severe problems than the worst case winds used for the FSL verification. The flight rule requiring manual bank maneuvers in this Mach region following RCS jet failures also tended to alleviate the problem. Based on the results of the verification process the GN&C community had a high degree of confidence as the Orbiter entered the flight test program.

FLIGHT TESTING CHALLENGE

Stability and control testing of the Space Shuttle is driven by conflicting program desires, while limited by unique problems. Space Shuttle flights are very costly when compared with test flights of other aircraft. There is an intense desire within the program to bring the Shuttle to an operational mode, where payloads can begin to make the Shuttle cost effective. On the other hand it is important to assure the safety of entry flight and to identify the real limitations of the Shuttle through flight testing. This conflict in goals has resulted in the need for a minimum amount of highly productive testing.

Conventional flight test techniques and computer programs have formed the basis for the Shuttle flight test program. Modifications to these techniques have been necessary, however, due to the inherent constraints in Shuttle testing. Measures have been taken to ensure the quality of maneuvers and the data from them, so that the number of repeat maneuvers can be minimized.

The flight test plan developed for the Shuttle contains very few test points when compared to test programs of military aircraft. Enough maneuvers are scheduled only to verify the safety of the Shuttle entry; not enough to build a flight test data base. Where significant differences exist between the flight data and the wind tunnel data base, further test points are scheduled.

The stability and control derivatives are obtained from the onboard sensor data through the MMLE3 parameter identification program.[9] This program was developed at Dryden Flight Research Facility and is a state-of-the-art method of extracting derivatives from flight data. MMLE3 is the latest version of a program which has been used in many test programs for all types of aircraft.

Derivative deltas calculated between flight and values from the Shuttle Aerodynamic Design Data Book[10] are provided to Shuttle simulators to demonstrate the safety of further testing on upcoming flights and to assure the safety of flying cg's associated with planned payloads.

TEST REQUIREMENTS

Aerodynamic test requirements have arisen from two sources. The original source is the preflight wind tunnel data and the associated aerodynamic variations. The other source of requirements is the flight data from the initial flights, during which anomalies occurred. The types of problems identified involve either potentially excessive RCS fuel usage for longitudinal and lateral trim, or potential loss of control.

PREFLIGHT TEST REQUIREMENTS

Preflight wind tunnel data for the Orbiter is very extensive and coupled with the FCS verification process provided sufficient confidence to fly the initial missions under benign conditions and within a limited range of x cg[11]. However, at the cg extremes, analysis indicated

combinations of uncertainties in pitching moment and the stability and control derivatives resulted in potential control problems. These potential problems resulted in the establishement of the entry flight placards on angle of attack, dynamic pressure and x cg mentioned previously. Figure 12 shows the preflight areas of concern identified on a typical Mach-alpha profile.

From entry interface to a dynamic pressure of 20 lbs per sq ft, uncertainties in basic pitching moment and in pitch jet, bodyflap, and elevon effectiveness indicated a possible problem in longitudinal trim at the cg extremes. Such a trim problem would result in excessive use of RCS fuel by the pitch jets.

From Mach 7 to 3, uncertainty in the LCDP was the primary concern. Since the LCDP changes signs in this Mach region, the FCS gains were designed to provide a transition from a mode requiring a negative LCDP to a conventional aircraft control mode requiring a positive LCDP. Since the exact location of the sign change in the LCDP is unknown there is a requirement for identifying the aerodynamic coefficients in the LCDP and determining the effects of the elevon and cg position on these coefficients.

In the region from Mach 3 to 1, C_{n_β} dynamic was a concern, particularly for trajectories resulting in large dynamic pressures. C_{n_β} dynamic was also a concern in the Mach 5-8 region for high wind cases that produced an error in the navigation derived angle of attack. After the rudder becomes active at Mach 3.5, the combined lateral trim characteristics of the aileron and rudder were of particular interest.

Flight testing is planned between Mach numbers of .9 and .75 due to reduced rudder effectiveness at minimum speedbrake settings. The rudder is aft of the maximum thickness point on the vertical tail, and effects of the flow past the rudder panels become less certain with a closed speedbrake.

FLIGHT TEST REQUIREMENTS FROM FLIGHT DATA

Anomalies in the actual flight data have extended the test requirements as originally conceived. These anomalies have in some cases accentuated the need for certain data already in the flight test plan. Others have pointed to a need for more concentrated investigation of certain flight regimes. A summary of flight anomalies are shown in figure 12, items 1 through 7.

During the initial bank maneuver on flight 1, at a dynamic pressure of 14 lbs per sq ft, a large oscillation occurred in sideslip. Studies have indicated that the primary cause was a missed prediction in roll due to yaw jet firing.[12]

Another flight anomaly is a longitudinal trim difference from what was predicted. This occurs both in the hypersonic regime with a pitch up difference and in the transonic regime, where the difference is a pitch down moment.[12] Because the pitching moment anomaly causes more up (-) elevon trim transonically, the aileron effectiveness data required in this regime has become even more important. The hypersonic anomaly has caused an increased need for longitudinal stability and control data to ascertain the contributions of $C_{m_{\delta_e}}$, $C_{m_{\delta_{BF}}}$, C_{m_α}, and C_{m_o} to this problem. Figure 13 indicates the range of elevon settings required for trim based on attributing the pitching moment difference to C_{m_o} alone.

Causing additional interest in the Mach 2 to 1 regime is an anomaly which has been observed on the first five flights. The anomaly is in the form of an undamped low amplitude roll oscillation, which has a frequency of approximately 1/4 hertz. This problem has not resulted in additional test requirements, since intensive testing is already planned for this regime.[12]

Additional stability and control testing in the hypersonic regime has resulted from STS-1 data. These data indicated that lateral stability was different than expected. Specifically C_{n_β} was more (+) than expected.[11, 13, 14] In addition, aileron trim was observed to have an offset between Mach 18 and 7. This offset has been observed to change signs, indicating possible flow asymmetries.

Another important anomaly has occurred hypersonically. Above Mach 10, where the elevon schedule has been varied between -1 and +5 on flights 1-4, the flight data indicate that the aileron is more effective than predicted at positive elevon deflections. The data also indicate the effectiveness to be close to nominal at 0^{o} elevon setting. While this is beneficial for positive deflections, the trend indicates that the aileron may be less effective at negative deflections. This accentuates the need for data which will clarify the dependence of aileron on elevon deflection.

These anomalies have not restricted the flight placards further. However, they have emphasized the need for data in certain flight regimes. They have also caused the planning of further testing in specific areas.

SHUTTLE FLIGHT TEST PROGRAM

The Shuttle test program is the product of significant planning and integration with other program requirements. The flight test requirements from wind tunnel uncertainties and flight anomalies dictated the flight conditions at which maneuvers would be done. Sufficient maneuvers were planned at nominal conditions to indicate repeatability of results. Additional maneuvers were planned over the ranges of elevon and angle of attack that will be seen operationally to check coefficient sensitivities to these parameters. The test plan has been modified to provide additional information in areas where anomalies have occurred. This is necessary to establish an understanding of the anomaly and to develop a data base for simulators in areas where the wind tunnel data is deficient.

The tests planned for each flight are limited by the nature of the Shuttle entry and by other program requirements. Only one maneuver at each flight condition is possible on a given flight, since the Shuttle glides from 400,000 ft in altitude at Mach 25 to touchdown in the span of 30 minutes. The crew has monitoring functions and other tasks during entry that also limit the number of maneuvers that can be performed. This has resulted in a limit of 8 to 10 maneuvers per flight and in a ground rule which requires that maneuvers be spaced to the satisfaction of the flight crew. Another limitation is the amount of RCS fuel available for doing maneuvers. Entry tests must compete in priority with other mission objectives for RCS fuel. This includes on-orbit activities such as rendezvous tests and payload deployment. Other entry tests such as structural flutter tests and aerothermal pushover pullup test maneuvers (POPU) have taken priority over stability and control maneuvers, because instrumentation for these tests were available on flights 1-5 only. When a conflict occurs, guidance maneuvers and guidance phase changes take priority over test maneuvers.

The flight testing has been planned to meet program objectives. The first and most important is to open the cg placards as quickly as possible in order to verify the safety of flying planned payloads. In addition, data resulting from tests are scheduled to support planned flight control system changes which will improve control where in-flight aerodynamic anomalies have occurred.

SENSOR DATA FOR TESTING

Sensor data used in stability and control analysis is obtained from two basic sources. The primary source of data is the aerodynamic coefficient identification package (ACIP), which is located in the wing carry-through structure. It was designed specifically for aerodynamic data extraction. The other source is the onboard data system, which provides real-time data for the guidance and flight control systems. The ACIP is a high quality data package recording data at 173 samples per second utilizing a 14 bit system. The onboard data system records data at 5 and 25 samples per second using an 8 bit system. A more detailed explanation of the sensor data is given in reference 12.

STABILITY AND CONTROL MANEVUERS

Maneuvers for stability and control data have been carefully developed to provide the maximum amount of information possible. It is important in this testing to excite the motion defined by the derivatives in question, so as to identify them from the flight data. Because of the limited testing of the Shuttle and the characteristics of the flight control system, precise maneuver design and execution are very important. Poorly performed maneuvers can be costly to the program in the form of further required testing.

The flight control system of the Shuttle heavily modifies inputs through the stick and is designed to damp oscillations and transients. This design causes difficulty in pulsing a control effector and allowing motion to damp as is done with most aircraft. In pulsing the Shuttle, the

control system modifies the stick input with filters, responds to rate and acceleration feedback values, and damps the response with further surface motion. In general, when the vehicle is pulsed, all control effectors available are put into action to quickly damp the vehicle motion. This can cause difficulty in separating out the effectiveness of the various control effectors. It makes it difficult to accurately identify damping derivatives.

To overcome this important problem and to provide exact designed inputs, programmed test inputs (PTI) were developed. This type of maneuver is input directly to the flight control system through onboard software. The amplitude and timing is governed by programmed variables to generate a specific input at a predesignated flight condition.

The crew involvement in the maneuvers is almost entirely a monitoring function. The maneuver sequencing is initiated by the crew before the first maneuver, and the software automatically executes the predefined maneuvers within specified windows. These windows are defined by dynamic pressure or Mach number. The software avoids executing maneuvers close to bank reversals and other guidance phase changes. The crew monitors trajectory and trim parameters and important entry flight systems to assure safe maneuver conditions. The crew can quickly stop the maneuver sequence by moving the stick or selecting the control stick steering (CSS) mode. They have full visibility into the testing status through items on their displays.

The inputs are made through the flight control system, and go to an integrator at the point where the surface deflection is commanded. The input is added to the current command. The command, a surface rate, is then processed through a maximum rate limit function. Signals can be sent to the elevon, aileron, rudder, and pitch, yaw, and roll jets. Because of the direct input capability, maneuvers are input in the automatic guidance mode. The input is in the form of a doublet. The doublet commands surface rate in one direction and then the opposite direction resulting in a pulse from the control effector. These doublets can be strung together in combinations to provide various inputs from each of the control effectors. There is a capability to define 25 PTI windows, and there are 45 doublets that can be grouped in the windows as desired.

The input from the automatic PTI is not completely free of flight control system interference, but the design does allow for enhanced maneuvers. An example of a maneuver for Mach 5.8 is illustrated in figure 14. The inputs are defined by amplitudes, times, and the effector to be pulsed. The flight control system continues to respond to the motion feedback, but direct input can be made to the control effector. In this example it is possible to make the aileron input while there are no yaw jet firings.

Direct input to the surfaces in a "bare airframe" sense is not possible in the program at present. With the basic lack of stability of the Shuttle, it would not be safe to maneuver the vehicle without an active control system. The automatic PTI design offers the most feasible alternative that is available.

Maneuvers, once designed for the optimum motion for data extraction, are assessed for flight control and guidance safety. Although potential problem areas are approached carefully, care must be taken in maneuvering not to excite an undamped or diverging oscillation. It is also important not to perturb the trajectory so as to disturb the ranging capability during the Shuttle's gliding descent.

Maneuvers are studied extensively for flight control safety. Both off-line and real-time simulators are used to study maneuvers with worst case aerodynamic uncertainty combinations. Maneuver amplitudes are increased to assess safety margins. Loss of RCS jets is also simulated. Flight test aerodynamic results are fed through this same process to verify maneuver safety margins with data that is the best possible representation of actual Shuttle characteristics.

Maneuver guidance impacts and entry timeline conflicts are assessed in a similar manner. Simulations are run to determine conflicts between stability and control maneuvers and guidance maneuvers and phase changes. Shuttle pilots assess maneuver conflicts with other important pilot functions. If conflicts arise from these studies, maneuver windows are adjusted or are deleted. In general the short, low amplitude, PTI maneuvers have a negligible impact on guidance capability, but they are studied nonetheless. When combined with other maneuver sequences, guidance impacts can occur. RCS jet fuel budgets for maneuvers are developed during these simulations to provide the pilots with fuel "red lines" that must not be violated, in order to continue initiating maneuvers. Usage of RCS fuel during maneuvers is significant. Loss of vehicle control is possible if the RCS fuel is depleted.

SHUTTLE MANEUVER TEST PLAN

The maneuvers planned or already flown on each flight are listed in figure 15. The left hand column lists the flight conditions at which the tests are planned. The other columns are labeled by flight number. Flight one had no planned maneuvers other than bank reversals required for ranging. The first entry was designed to be as benign as possible. Flight 2 had 25 maneuvers, including pitch and roll maneuvers for stability and control data, a pushover pullup maneuver, and bodyflap pulses. Subsequent to STS-2, decisions were made to reduce the number of maneuvers per flight so as to decrease crew workload during entry. As a result fewer maneuvers are shown on flights 3-17. The test program has therefore evolved from an initial 10 flights into a 17 flight program in order to obtain sufficient data. It can be observed in figure 15 that the most concentrated testing is from Mach 6 to .9. This is because it is the most critical regime with respect to potential problems in stability and control.

The test plan for stability and control data is designed to provide sufficient information to remove forward and aft cg constraints. The forward center of gravity travel is limited primarily by aileron characteristics at negative elevon settings. To verify the aileron characteristics before flying a forward cg, the vehicle trim of a forward cg is simulated by appropriate scheduling of the elevon. Elevon schedules for flights 1-17 are shown in figure 16 with the locations of the maneuvers from figure 15 superimposed. The schedules cover the range of expected values for the full range of cgs. These elevon schedules are attained during flight by onboard software programming of the elevon settings. The bodyflap is used to trim the vehicle at the given setting. The schedule shown for flight 2 is the most benign schedule and provides the most positive aileron control between Mach 6 to 1. As the flights progress and more data is obtained, the elevons are to be scheduled gradually more up (-) until the most forward cg is simulated on flights 14-17. Hypersonically, the elevon is being trimmed beyond what is required during normal entry for a forward cg (figure 13). This is due to the data already obtained which indicated anomalous aileron effectiveness as a function of elevon position. The settings shown on flights 14 to 17 should shed additional light on this problem and the results can be used to assess certain abort profiles which use more negative elevon positions for trim.

Angle of attack will be varied on a limited number of flights. Figure 17 illustrates the nominal angle of attack profiles to be flown on particular flights. Maneuvers will be executed along these profiles to verify predicted angle of attack trends in stability and control parameters. Flights 6, 8, and 12 will be flown with an elevon schedule that has been flown previously so as to vary only one parameter at a time. Flights 14, 16, and 17 will be flown with an elevon setting that represents the trim requirements for a forward cg. The symbols represent where maneuvers will occur along the profile on flights where the profile is off-nominal. Stability derivatives C_{ℓ_β} and $C_{n_{\delta_A}}$ are of particular interest as a function of angle of attack. In addition, an understanding of the possibility of aileron effectiveness being a function of the combined effects of angle of attack and elevon is to be studied. This will require deviations in both angle of attack and elevon position for various maneuver test points.

Additional factors in the planning will contribute to the necessary understanding of the stability and control characteristics of the Shuttle. Figure 18 shows speedbrake schedules for the nominal entry, and planned schedules for flights 5 through 17. With these different schedules, rudder sensitivities can be obtained. With the automatic maneuvers beginning on flight 5, a rudder pulse can be input at any point regardless of whether or not the rudder is active in the flight control system. The rudder normally becomes active at Mach 3.5. With this capability, the rudder effectiveness will be tested 1/2 Mach number higher per flight, beginning on flight 5 at Mach 4. To obtain further data on possible aerodynamic asymmetric characteristics of the Shuttle, Ycg offsets are planned through payload placement. Ycg values of .5 to .9 inches have been flown on flights 4 and 5. A Ycg value of 1.5 inches is planned for flights 7 and 11, with the sign of the offset reversing between the two flights. Although POPU maneuvers were planned primarily to obtain aerodynamic performance and aerothermal data, these maneuvers were also a valuable source of additional longitudinal stability and control data. Bodyflap pulses were flown only on STS-2. During these maneuvers the crew manually changed bodyflap trim down (+) to move the elevons up (-). A PTI was then performed. This was to provide early indications of aileron effectiveness with more (-) elevon settings.

FLIGHT DATA ASSESSMENTS

An important product of the flight test program is the confidence that is gained from flight test results, in assessing the safety of upcoming flights. Vehicle cgs associated with specific payloads must be shown to be safe. In addition, further testing in the flight test program depends on values of derivatives obtained from previous tests. For instance, it is important to

understand as much as possible about stability and control characteristics for down elevon positions, before it is safe to fly with elevons at more negative settings. To accomplish this, fairings are developed for the flight test results and are provided to the Shuttle flight control system community. These fairings or "assessment" values are incorporated into simulators which are used to verify the safety of upcoming flights. Exact maneuvers and trajectory profiles are simulated with correct cgs. In addition, stability analyses are performed using the flight derived aerodynamic data to update cg placards for the vehicle.

STS-1 THRU -4 FLIGHT ASSESSMENT VALUES

Flight test results in the form of stability and control derivatives have been output for use in simulators after flights 1, 2, and 4. Some of the most significant of these derivatives are shown in figures 19 to 24. These figures show derivative values for various types of maneuvers from flights 1 to 4. It is important to note that the highest quality maneuvers are the PTI's, which have darkened symbols. In the plots, pre-flight 1 Aerodynamic Design Data Book values (solid line) and the associated uncertainties are drawn. The abrupt changes in the data book values at some locations are due to the data being plotted for the specific flight condition and configuration where the maneuver was executed and do not represent abrupt nonlinearities in the data base. The uncertainty brackets on the derivatives are Cramer Rao bounds, which provide information on the relative accuracy of data extraction between data points.[9] Also drawn on the plots are the STS-4 assessment values. These assessment values are the fairings that have been published from flights 1 to 4 for these derivatives.

For C_{ℓ_β} in figure 19, the flight test values are shown to be significantly more positive than what was predicted above Mach 10. However, this is of no particular concern to the safety of the Shuttle through this Mach regime. Below Mach 6 the C_{ℓ_β} fairing is shown to be approximately halfway between nominal and the lower value of the uncertainties. This value of C_{ℓ_β}, by itself is not of concern for for Shuttle safety of flight, but if $C_{n_{\delta_a}}$ should become positive for more up elevon settings, the more negative C_{ℓ_β} will have an adverse effect on the LCDP.

Aileron effectiveness above Mach 10 is shown for PTI's in figures 20 and 21. These values are plotted as a function of elevon position. Because of the spread of elevon between flights 1 through 4 in this Mach regime, a difference in the effect of elevon on aileron effectivness has been discovered. Both $C_{\ell_{\delta_a}}$ and $C_{n_{\delta_a}}$ indicate increased effectiveness with down elevon deflections. The assessment values for elevon settings above 0^o were set to nominal, because of the lack of data. If the trend for positive elevon deflections extend to negative elevon deflections, the aileron may be less effective than predicted. Although this difference between predicted and actual aileron effectiveness has little effect on safety hypersonically, the impact to cg placards could be important if the trend continues at lower Mach numbers. Testing on later flights, where the elevon will be scheduled with more negative settings, will provide the necessary data to determine Shuttle cg impacts. This example points out the importance of obtaining derivative sensitivities to elevon and angle of attack profiles. Between Mach 2 and 1 (figure 22) the flight values of roll due to aileron are shown to be less effective than predicted. In this region the elevon has been above 0^o deflection due to overshooting the elevon schedule. Because there has been no spread in the elevon deflections on flights 1 to 4, it is not yet possible to attribute this anomaly to effectivness due to elevon position. Later flights will provide the spread necessary to determine this function.

The most significant updates in stability and control aerodynamics are the assessment values and new uncertainties for yaw jet effectiveness. Figures 23 and 24 show very consistent flight test results for RCS yaw jet effectiveness. After STS-4 sufficient data was available to update nominal values and reduce RCS jet effectiveness uncertainties from early entry through Mach 1, where the yaw jets are turned off. The jets were shown to be more effective than predicted. These results have had a significant effect on cg expansion.

CENTER OF GRAVITY EXPANSION

The primary goal of the entire data extraction effort is to open cg placards for the Shuttle, so that the full payload carrying capability can be utilized. Through the planned maneuvers, and

elevon and angle of attack schedules, sufficient data is to be obtained to verify the Shuttle operational safety during entry. The operational limits for cg have been specified to be from 65 to 67.5 percent of the reference body length. This represents a cg travel of 32.32 inches. It is the goal of the test program to relax cg placards to these operational limits. Figure 25 shows the expansion of the Xcg that has taken place as a result of flight test data from STS-1 thru -4. Opening of the aft cg boundary as well as initial opening of the forward boundary is primarily a result of the confidence that has been gained in the knowledge of the basic pitching moment of the vehicle. Pitch jet trim requirements were also determined. The most restrictive boundary is the forward cg limit, because of the critical potential problem areas between Mach 6 and 1. The most significant relaxation of this forward boundary occurred because of the yaw jet flight test results. The more effective jets along with the reduced uncertainties resulted in the change shown in the placard between STS-5 and -6. This has proved the safety of flying payloads planned for STS-7 and -9. Also shown in figure 25 are aft cg flight test limits, which must be honored in order to fly the elevon schedules planned for these flights. Relaxation of the boundary to the full forward limit of 65 percent body length will occur as a result of decreases in other stability and control derivative uncertainties by the end of the flight test program. Optimistically these data will prove that predicted potential control problems do not exist.

CONCLUSIONS

The successful flight of STS-1 in April 1981 proved that the challenge of the FCS design and verification has been met. The flight test data so far is indicating that the aerodynamic variations were not overly conservative, but are representative of the actual differences experienced in most of the aerodynamic coefficients at some point during reentry. The successful extraction of flight test data from the first four flights is proving that the challenge of developing an operational vehicle with a minimum flight test program is being successfully met.

The placards on the orbiter during entry are to be reduced after 17 flights based on high quality data from carefully designed manevuers. The approach is optimistic and ambitious but every effort is being made to insure its success through careful maneuver design, quality data and safety analysis. The experience gained and techniques employed in the Shuttle program are applicable to future flight test planning in programs where testing must be limited due to time constraints or expense.

REFERENCES

1. Young, James and Underwood, Jimmy: The Development of Aerodynamic Uncertainties for the Space Shuttle Orbiter, AIAA Paper 82-063.

2. Weil, Joseph and Powers, B. B.: Correlation of Predicted and Flight Derived Stability Derivatives with Particular Application to Tailless Delta Wing Configurations, NASA TM-81361.

3. Kanipe, David B.: Plume/Flowfield Jet Interaction Effects on the Space Shuttle Orbiter During Entry: AIAA Paper 82-1319, August 1982.

4. Gamble, J. D. and Young, J. C.: The Development and Application of Aerodynamic Uncertainties in the Design of the Entry Trajectory and Flight Control System of the Space Shuttle Orbiter, AIAA Paper 82-1335, August 1982.

5. Weissman, R.: "Status of Design Criteria for Predicting Departure Characteristics and Spin Susceptibility," J. Aircraft, Vol. 12, No. 12, Dec. 1975. pg. 989-993.

6. Kaylor, Jack T; Rowell, Lawrence F.; and Powell, Richard W.: A Real-Time Digital Computer Program for the Simulation of Automatic Spacecraft Re-entries, NASA TMX-3496, July 1977.

7. Rowell, Lawrence F.; Powell, Richard W.; and Stone, Howard W. Jr.: Development of the Re-entry Flight Dynamics Simulator for Evaluation of Space Shuttle Orbiter Entry Systems, NASA Technical Paper 1700, October 1980.

8. Bayle, G. P.: Entry Flight Control Off-Nominal Design Considerations, AIAA paper 82-1602CP, August 1982.

9. Main, Richard E. and Iliff, Kenneth W.: User's Manual for MMLE3, a General Fortran Program for Maximum Likelihood Parameter Estimation, NASA TP-1563, 1980.

10. Aerodynamic Design Data Book, Vol. 1: Orbiter Vehicle, STS-1, Final Report, NASA CR-160903, November 1980.

11. Underwood, Jimmy M.; and Cooke, Douglas R.: A Preliminary Correlation of the Orbiter Stability and Control Aerodynamics from the First Two Space Shuttle Flights (STS-1 and -2) with Preflight Predictions. AIAA Paper 82-0564, March 1982.

12. Cooke, Douglas R.: Space Shuttle Stability and Control Test Plan. AIAA Paper 82-1315, August 1982.

13. Iliff, Kenneth W.; Maine, Richard E.; and Cooke, Douglas R.: Selected Stability and Control Derivatives from the First Space Shuttle Entry. AIAA Paper 81-2451, November 1981.

14. "Evaluation of the Space Shuttle Orbiter First Flight Descent Phase," AFFTC-TR-81-21, Office of Advanced Manned Vehicles, Air Force Flight Test Center, July 1981.

TABLE 1 ORBITER CORRELATION APPLICABILITY (REFERENCE 2)

AIRCRAFT*	GEOMETRIC FACTORS					REMARKS
	Δ WING PLANFORM	WING FLAP LONG. CONTROL	WING ELEVON LATERAL CONTROL	SINGLE VERTICAL TAIL	LARGE FUSLAGE	
XB-70	√	√	√			GOOD PRED BASE, M RANGE, CANARD, LIMITED α RANGE
YF-12	√	√	√			GOOD M RANGE, LIMITED α RANGE
X-15				√	√	WIDE α, M RANGE
TACT Λ = 58°	√			√	√	ONLY LIMITED DATA CURRENTLY AVAILABLE
HP115	√	√	√	√		LOW SPEED DATA ONLY
B-58	√	√	√	√		GOOD PREDICTIVE BASE, M RANGE
YF-16 F-8SCW				√		SOURCE OF RUDDER CONTROL DATA

*SEE REFERENCE 2 FOR AIRCRAFT IDENTIFICATION

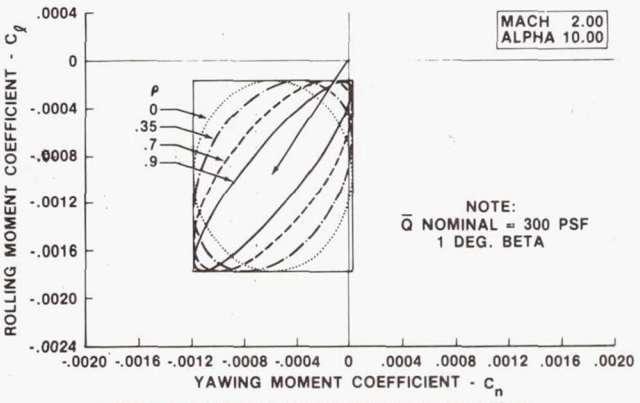

Figure 1. ELLIPTICALLY CORRELATED VARIATIONS

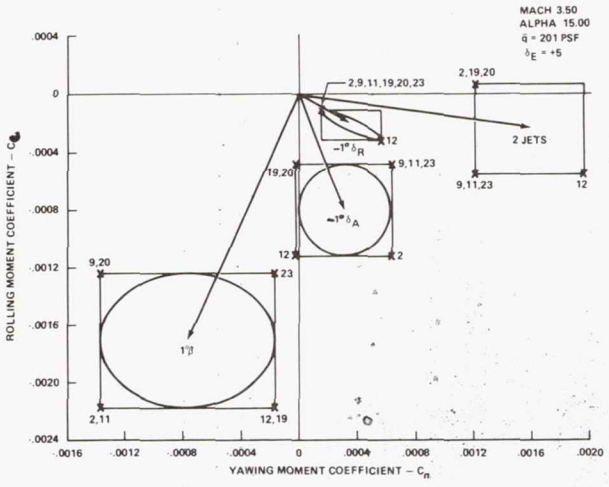

AERODYNAMIC VECTORS AT MACH 3.5 SHOWING VARIATION SETS

Figure 2. AERODYNAMIC VECTORS AT MACH 3.5 SHOWING VARIATION SETS

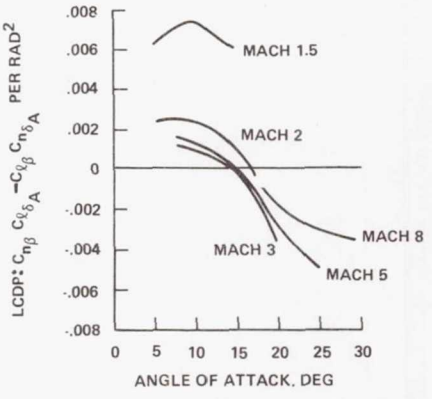

Figure 3. EFFECT OF ANGLE OF ATTACK ON LCDP FOR AERO VARIATION SET 19

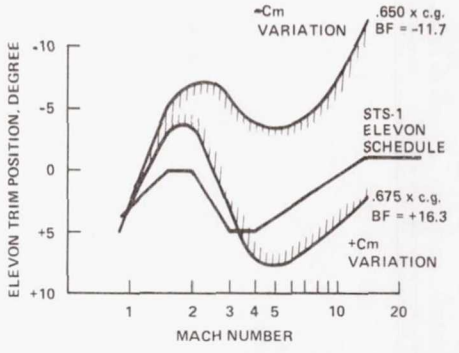

Figure 4. ELEVON TRIM ENVELOPE FOR DESIGN C.G. LIMITS WITH PITCHING MOMENT VARIATIONS

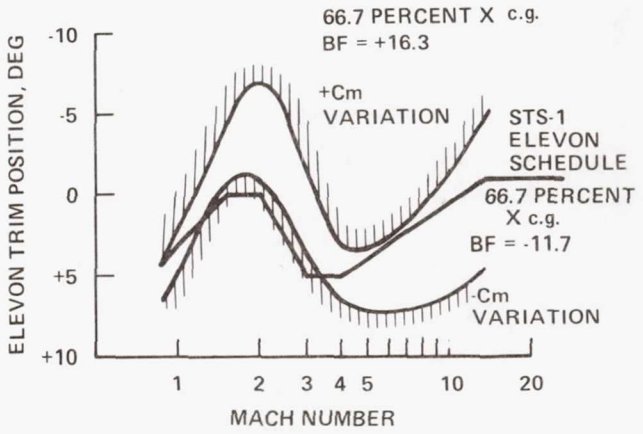

Figure 5. ELEVON TRIM ENVELOPE FOR 66.7 PERCENT L_B X c.g. WITH PITCHING MOMENT VARIATIONS.

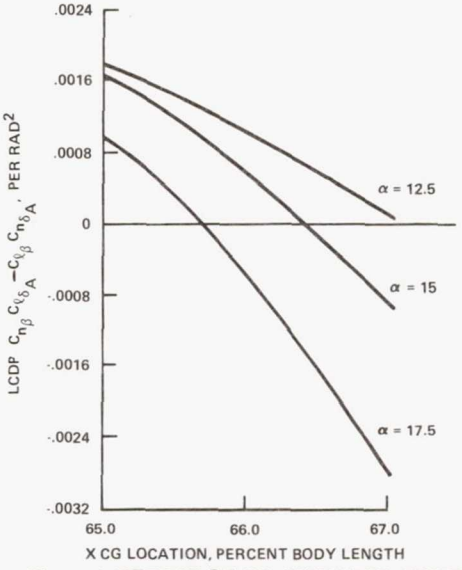

Figure 6. EFFECT OF CG, ANGLE OF ATTACK ON LCDP AT MACH 3.5 WITH AERO VARIATIONS SET 19

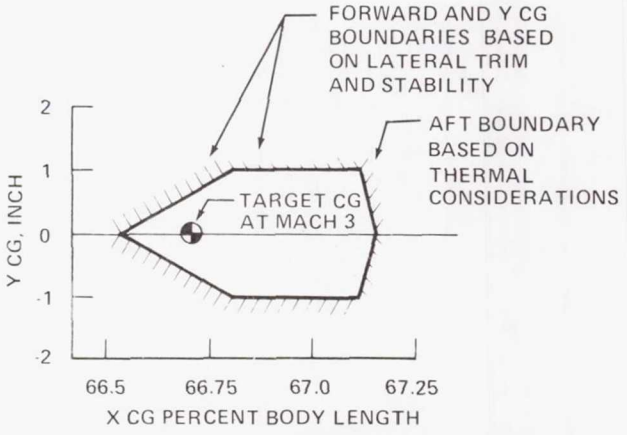

Figure 7. RECOMMENDED CG ENVELOPE CONTAINED IN FLIGHT RULES DOCUMENT FOR STS-1

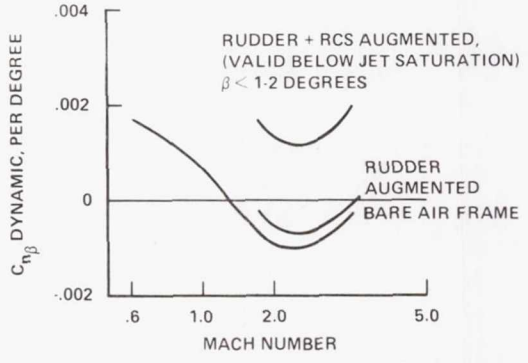

Figure 8. C_{n_β} DYNAMIC FOR WORST CASE VARIATION SET 1 g FLIGHT AT 7.5 DEGREES ALPHA

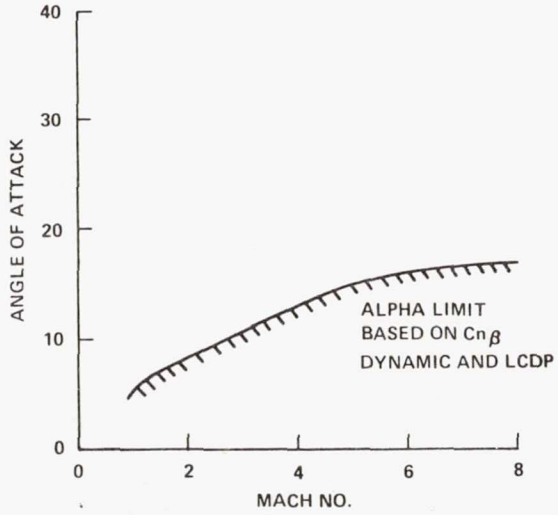

Figure 9. LOWER ANGLE OF ATTACK BOUNDARY CONTAINED IN FLIGHT RULES DOCUMENT FOR EARLY ORBITER FLIGHTS

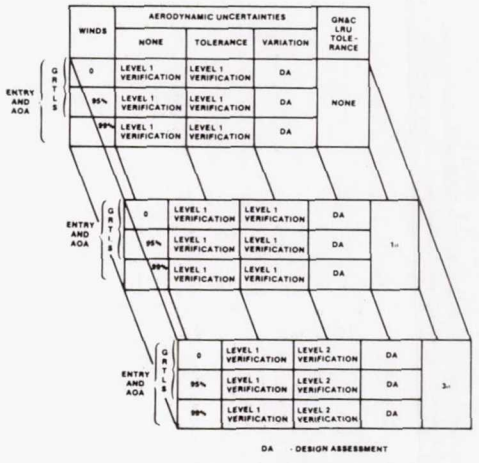

Figure 10. ENTRY VERIFICATION TEST MATRIX

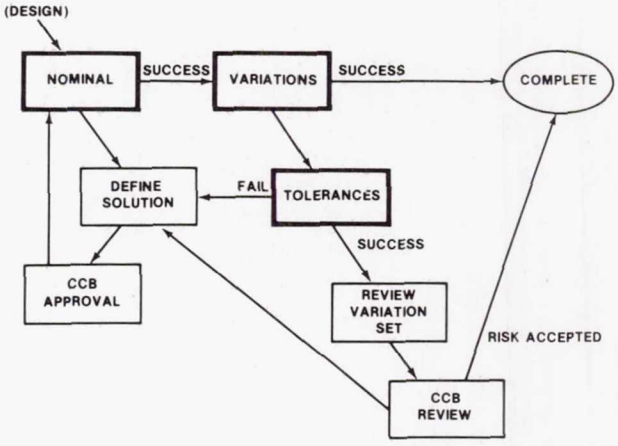

Figure 11. GN&C/FCS FORMAL VERIFICATION PROCESS

PREFLIGHT TEST REQUIREMENTS AND FLIGHT ANOMALIES

PRE-FLIGHT CONCERNS AT C.G. EXTREMES

A. VISCOUS TRIM AND LONGITUDINAL CONTROL (RCS FUEL,TRIM AUTHORITY)

B. LAT/DIR TRIM WITH ADVERSE $c_{n_{\delta_a}}$ (EXCESSIVE RCS FUEL,TRIM AUTHORITY)

C. LAT/DIR TRIM, CONTROL AUTHORITY WITH UNCERTAIN AILERON, RUDDER, JETS

D. LAT/DIR CONTROL AUTHORITY WITH UNCERTAIN AILERON, RUDDER JETS

E. LOSS OF RUDDER EFFECTIVENESS AND LAT STABILITY AT LOW SPEED BRAKE SETTINGS

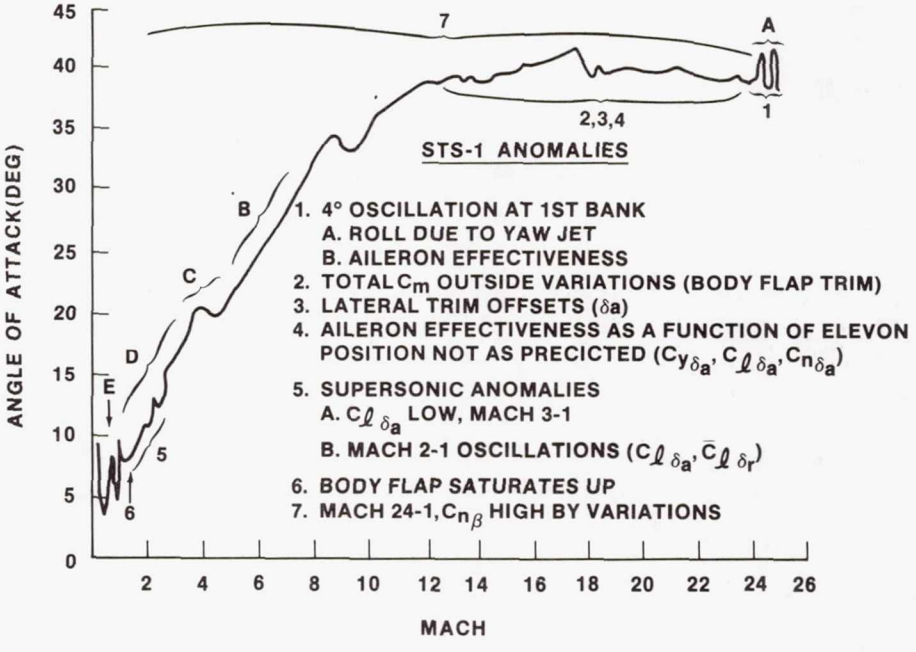

STS-1 ANOMALIES

1. 4° OSCILLATION AT 1ST BANK
   A. ROLL DUE TO YAW JET
   B. AILERON EFFECTIVENESS
2. TOTAL C_m OUTSIDE VARIATIONS (BODY FLAP TRIM)
3. LATERAL TRIM OFFSETS (δa)
4. AILERON EFFECTIVENESS AS A FUNCTION OF ELEVON POSITION NOT AS PRECICTED ($C_{y_{\delta_a}}$, $C_{\ell\,\delta_a}$, $C_{n_{\delta_a}}$)
5. SUPERSONIC ANOMALIES
   A. $C_{\ell\,\delta_a}$ LOW, MACH 3-1
   B. MACH 2-1 OSCILLATIONS ($C_{\ell\,\delta_a}$, $\bar{C}_{\ell\,\delta_r}$)
6. BODY FLAP SATURATES UP
7. MACH 24-1, C_{n_β} HIGH BY VARIATIONS

Figure 12

ELEVON TRIM CAPABILITY

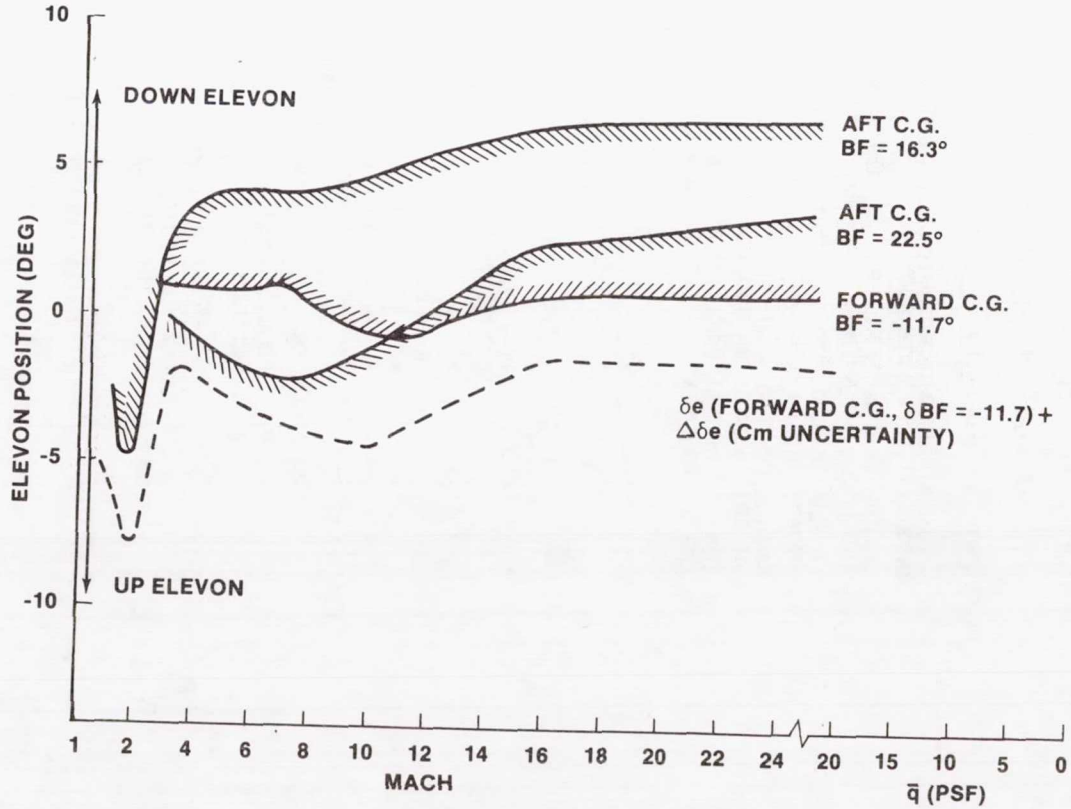

Figure 13

AUTOMATIC PTI CAPABILITY

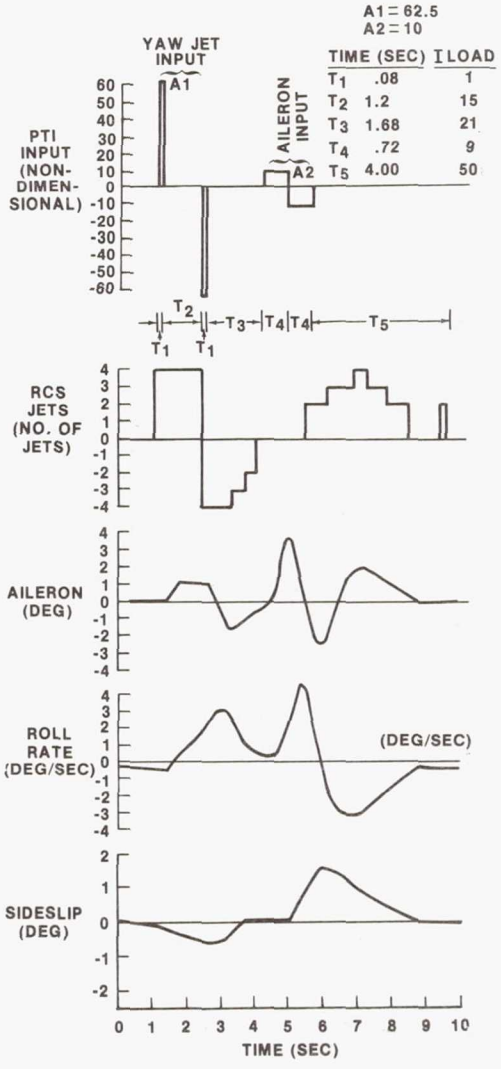

Figure 14

MANEUVER TEST PLAN

FLT # / FLT COND	1	2	3	4	5	6	7	8	9	10	11	12	13	14	15	16	17
q = .3		P															
q = 3		P							P								L,P
q = 4		L			L		L										
q = 8		L				L				L,P	L,P					L,P	
q = 10		P															
q = 16		P			~~P~~			P		L,P		L,P	L,P		L,P		L,P
q = 18		R															
q = 22		R	L	L	~~L~~	L		L	L				L		L		L,P
M = 21.5		P,L,BF POPU	L,P	L,P	L,P		L,P	L,P		L,P	L,P	L,P	L,P	L,P			
M = 18		L,BF	L	L	POPU	L,P	L,P	L,P		L,P	L,P	L,P	L		L,P		L,P
M = 15				L					L,P					L,P			
M = 14		L,BF	L	POPU			L,P			L,P	L	L,P	L,P				L,P
M = 8.4		L	L	POPU		L,P		L,P	L,P	L,P	L	L	L	L	L,P	L	L
M = 5.8		L			L	L	L	L	L		L	L		L	L,P	L	
M = 4.0		L	~~L~~		L	L,P		L	L				L	L	L,P	L	
M = 3.2		L		L	L	L	L			L	L	L	L	L	L	L	L
M = 2.2		L	S	S			L,P	L,P	L	L	L	L	L				L
M = 1.6		L		~~L~~	L,P	L		L,P	L	L,P	L,P	L		L	L	L	L
M = 1.1		L				L	L		L	L	L		L	L	L	L	
M = .9		L					L,P		L			L		L		L	

P - PITCH MANEUVER
L - LATERAL DIRECTIONAL
BF - BODY FLAP PULSE
POPU - PUSHOVER - PULLUP

S - STRUCTURAL PTI
~~L~~ - MANEUVER NOT EXECUTED

Figure 15

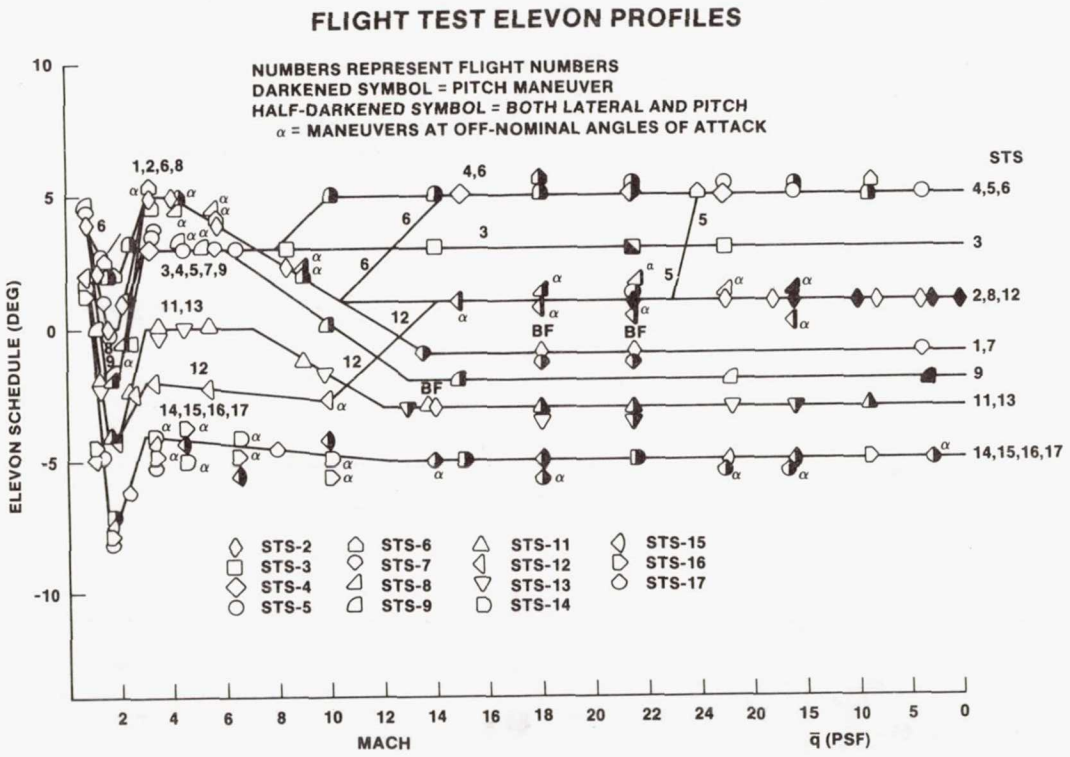
FLIGHT TEST ELEVON PROFILES
NUMBERS REPRESENT FLIGHT NUMBERS
DARKENED SYMBOL = PITCH MANEUVER
HALF-DARKENED SYMBOL = BOTH LATERAL AND PITCH
α = MANEUVERS AT OFF-NOMINAL ANGLES OF ATTACK
ELEVON SCHEDULE (DEG)
10
5
0
-5
-10
STS
4,5,6
3
2,8,12
1,7
9
11,13
14,15,16,17
1,2,6,8
3,4,5,7,9
11,13
12
14,15,16,17
4,6
BF
STS-2
STS-3
STS-4
STS-5
STS-6
STS-7
STS-8
STS-9
STS-11
STS-12
STS-13
STS-14
STS-15
STS-16
STS-17
2 4 6 8 10 12 14 16 18 20 22 24
20 15 10 5 0
MACH
q̄ (PSF)

Figure 16

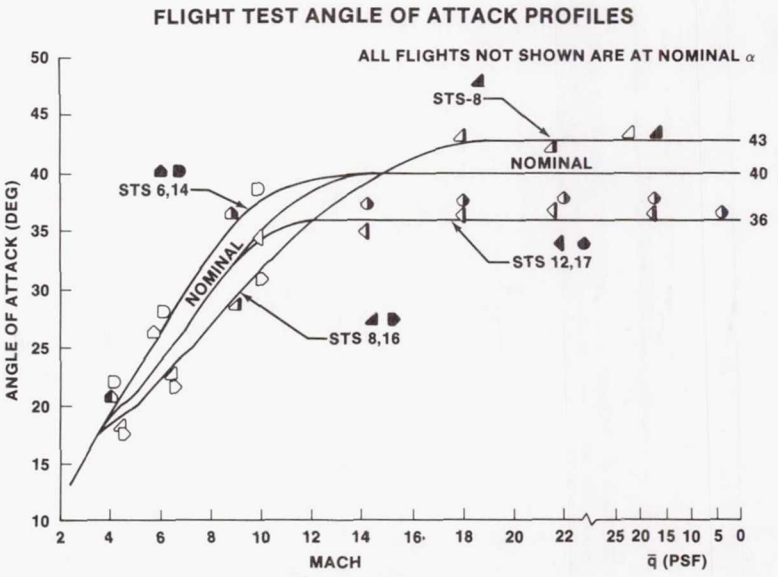

Figure 17

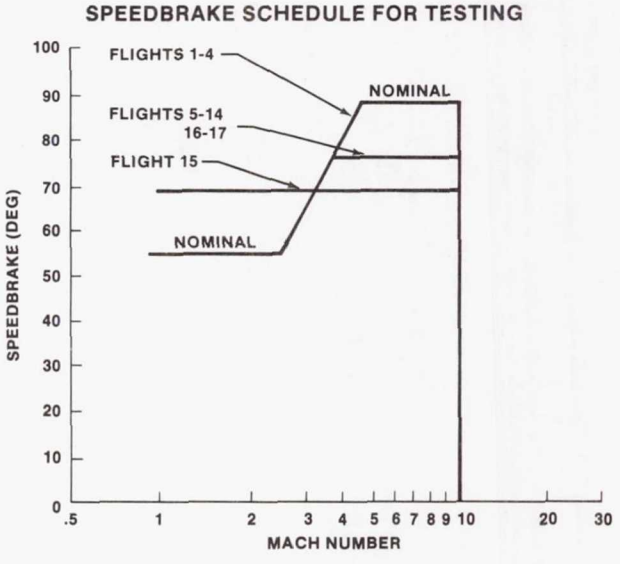

Figure 18

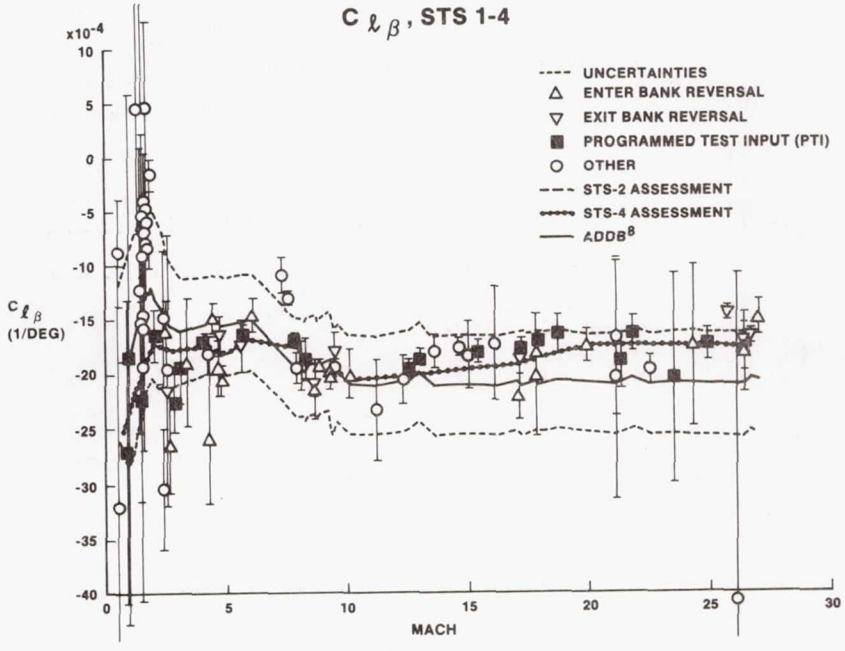

Figure 19

$C_{\ell_{\delta_a}}$ AS A FUNCTION OF ELEVON POSITION FOR M > 10, STS 1-4

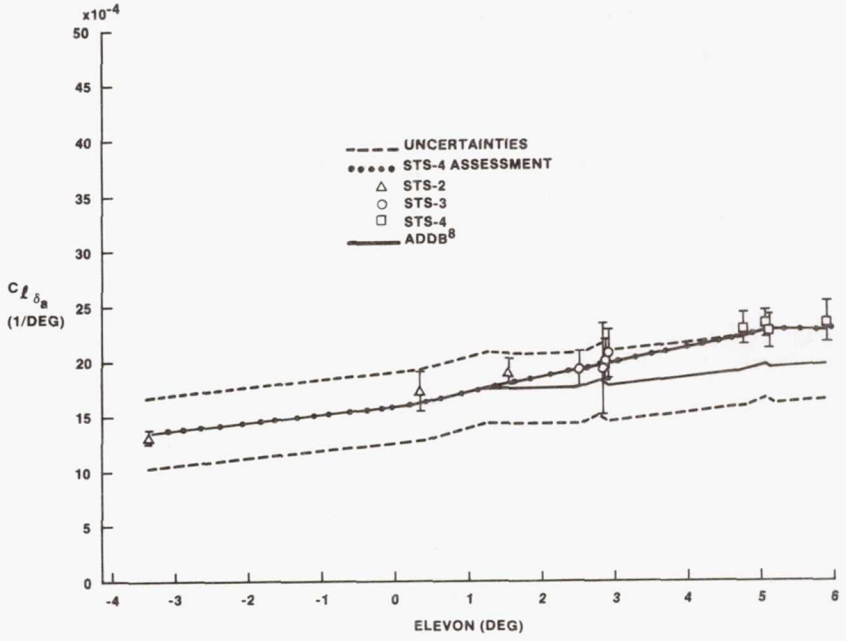

Figure 20

$C_{n_{\delta_a}}$ AS A FUNCTION OF ELEVON POSITION FOR M > 10, STS 1-4

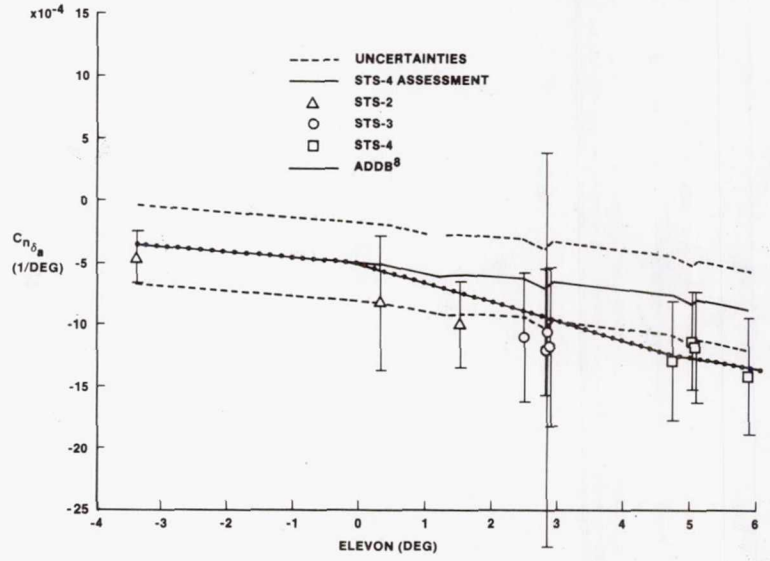

Figure 21

ROLLING MOMENT DUE TO AILERON, STS 1-4

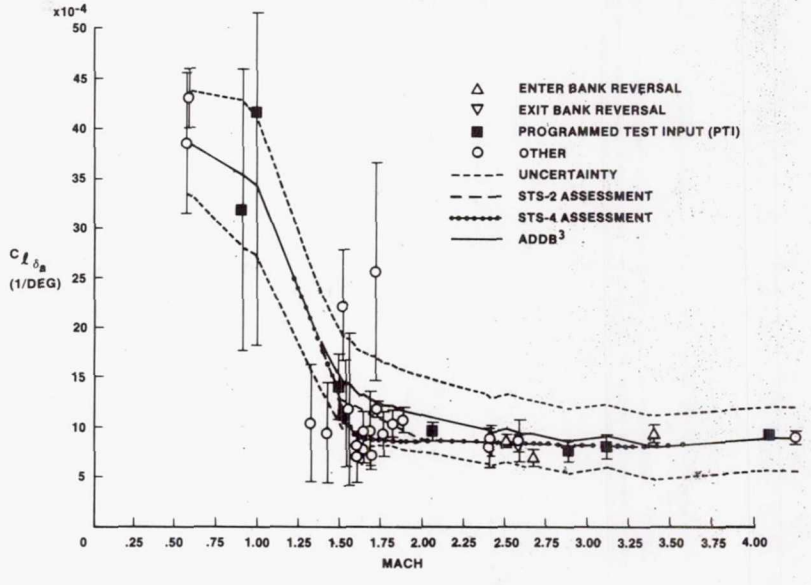

Figure 22

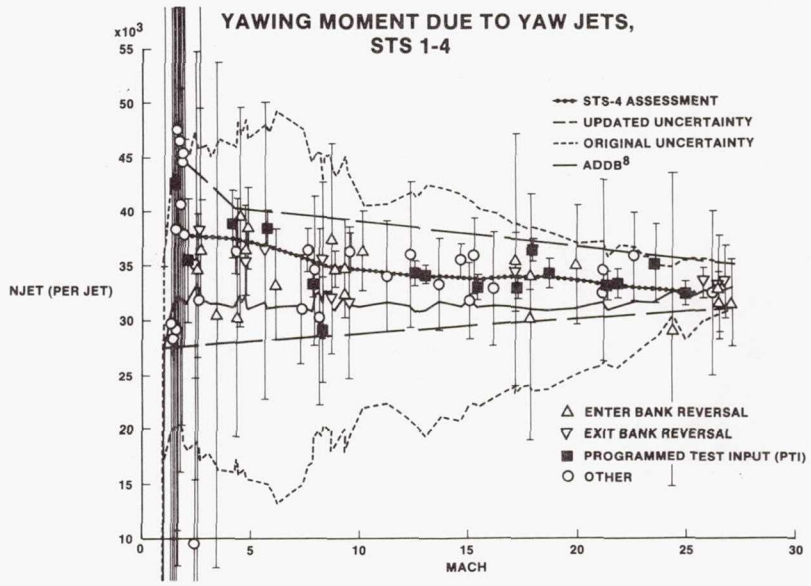

Figure 23

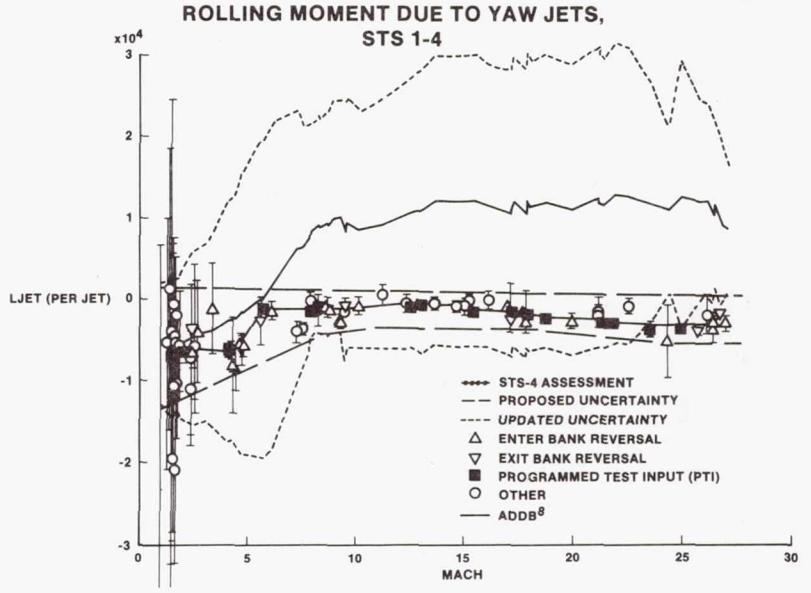

Figure 24

SHUTTLE CENTER OF GRAVITY PLACARDS (M = 3.5)

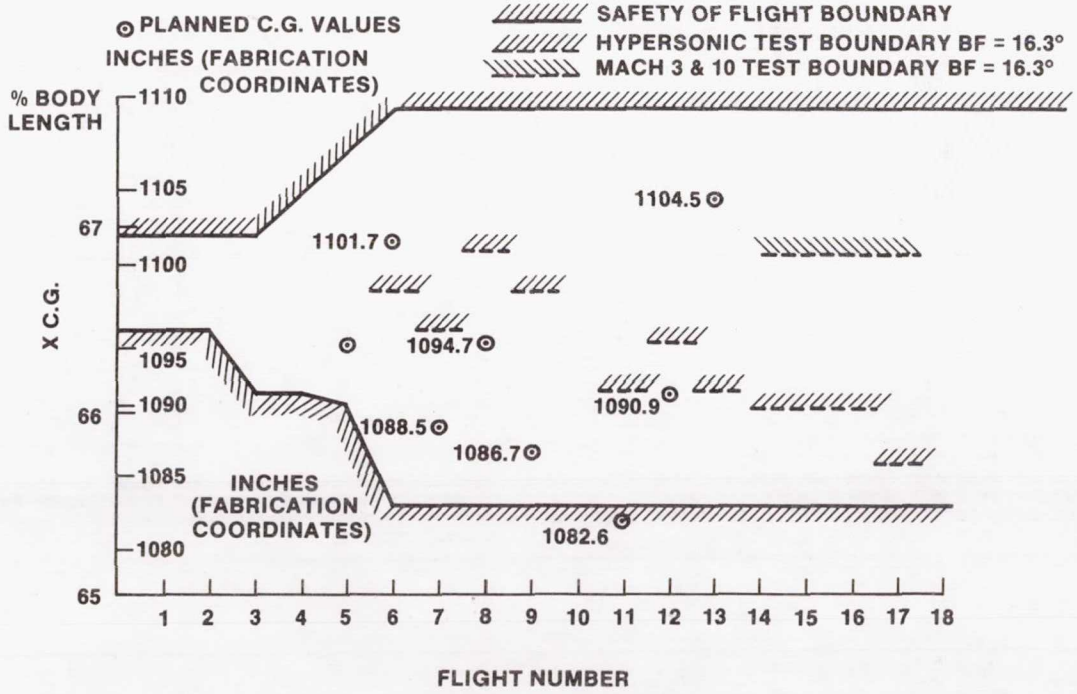

Figure 25